MECHANICAL PROPERTIES OF PAPERBOARD WITH A NEEDLED MIDDLE LAYER

MARIA KLINGBERG,[*] ANTAL BOLDIZAR[*] and KARIN HOFER[**]

[*]*Department of Industrial and Materials Science, Chalmers University of Technology, Gothenburg, Sweden*
[**]*Institute of Paper, Pulp and Fiber Technology, Graz University of Technology, Graz, Austria*
✉ *Corresponding author: A. Boldizar, antal.boldizar@chalmers.se*

Received October 21, 2017

Needling of formed kraft pulp at a dry content of 20% was previously shown to result in a redistribution of the fibres in the plane, resulting in local regions with a higher fibre structure density. The bending properties of a three-ply paperboard with a needled middle layer have been studied here, and it is shown that a needled middle layer can increase the bending resistance of a layered board by 8% and that the peak bending angle can be increased by up to 20%, although the bending stiffness may not be changed significantly. The needled middle layers had a higher compressive stiffness in the out-of-plane direction, but the effect of the needling on the tensile strength in the out-of-plane direction was insignificant.

Keywords: paperboard, needle punching, bending properties, folding, fibre network structure

INTRODUCTION

Conventional paperboard is a porous and anisotropic cellulosic structure, the anisotropic structure being primarily due to the flow of the pulp during manufacture, causing most of the fibres to be oriented parallel to the machine direction. Some fibres are oriented perpendicular to the direction of flow and in-plane, while only relatively few fibres are oriented in the out-of-plane thickness direction. The anisotropic fibre structure influences the stiffness, as well as the mechanical properties in general. The stiffness in the machine direction is often 1-5 times greater than in the cross-direction and up to 100 times higher than in the out-of-plane direction.[1]

The fibre network structure of paperboard is known to be important for many properties, such as the bending properties, and also for the performance of the board in converting operations, such as creasing, folding and printing.[2-4] The need for a three-dimensional fibre network structure has been discussed in the literature, as it is well understood that fibres oriented in the thickness direction promotes the in-plane compression strength, the bending stiffness and the out-of-plane strength of the board.[2,5,6] It is commonly understood that the strength and number of fibre-to-fibre bonds, the fibre stiffness and the strength in the transverse direction are the primary parameters governing the mechanical properties of the paperboard, but entanglement of the fibre network is also expected to be of importance.[7-9]

Studies of handmade sheets consisting of 90% eucalyptus pulp and 10% carbon fibres oriented in the thickness direction have shown that the out-of-plane shear strength was 14% greater than that of sheets made of 100% eucalyptus pulp, while the tensile strength did not decrease.[3] Fibres oriented in the out-of-plane direction have also been obtained by modifying the flow in the headbox and by the formation of high consistency, as a higher consistency reduces the anisotropy of the fibre structure, as this can increase the bulk and internal strength.[5,10]

The motivation of the present work was to explore the possibilities of improving the mechanical behaviour of paperboard by changing the fibre structure using the needle punching method. Specifically, the aim was to study the mechanical properties of a paperboard with three layers, where the middle layer of the paperboard was needled with different needle configurations

and the outer layers were conventionally produced. The mechanical properties of interest were mainly bending stiffness and folding resistance, as well as tensile strength and compression properties in the thickness direction.

The conventional needle punching method, commonly used in the textile industry since 1870, is basically used to achieve mechanical entanglement of long fibres in the dry state and to produce a non-woven multi-layered structure. The needles used are generally equipped with barbs in order to hook up the fibres and transport them in the thickness direction. Needle punching thus rearranges and entangles the fibres, primarily reorienting them in the thickness direction.[11] The needle punching performed in this work differs from the conventional needling of textiles in that it was performed on wet fibres with a length of 2 mm, whereas conventional textile fibres subjected to needling are normally at least 40 mm long.

The structure of needled cellulose fibre networks, needled with and without barbs, has recently been examined by several microscopy techniques.[12] It was concluded that the structure of the fibre network close to the needle penetration was densified with an in-plane redistribution of fibres. In the specimen needled with barbs, a few fibres were also oriented in the thickness direction.

EXPERIMENTAL

Materials

Unbleached softwood pulp was used for the middle layer of the three-layered paperboard, and bleached kraft pulp, consisting of approximately 15% hardwood and 85% softwood, was used for the outer layers. The average length and thickness of the bleached kraft pulp fibres were 1.9 mm and 27 µm, respectively, while those of the unbleached kraft pulp were 2.1 mm and 29.1 µm, respectively, measured in the production process with a PulpEye device.[13]

The volumes and concentrations of the pulp stock were chosen in order to obtain a grammage of 140 g/m^2 for the middle layers and 100 g/m^2 for the outer layers, and the stock was stirred in a beaker for at least 10 minutes. A laboratory handsheet former (SCAN CM-26:9) was used to make all the sheet samples according to EN ISO 5269-1. The sheets produced were then kept at dry content of 20%.[12]

Needling method

The middle layers were needled with a laboratory needling machine of the DI-LOOM OUG-II SB15 type at Groz-Beckert KG, in Germany, at 23 °C and 42% relative humidity. The dry content of the samples was measured to be 20 ± 5% before needling. The needle punch machine was equipped with a needle board with 1000 needles, having barbs of the 15X18X43X3 R222 G 2017 type. The length of the triangularly shaped cross-section of the needle part in work was 20 mm with a cross-section of 0.40 mm. Two barbs were positioned on each of the three edges at a distance of 6.36 mm from each other. The distance between barbs on different edges was 2.36 mm. Only the three barbs close to the needle point were used in this study.

The middle layers were passed through the needle punch machine, where the needles penetrated the sheets by a vertically oscillating movement of the needle board. With a needle penetration depth of 4, 6, 8 or 10 mm, the numbers of barbs penetrating the samples were zero, one, two or three, respectively. The needle stitch densities used were 40 or 60 stitches/cm^2, denoted low (L) or high (H). For each stitch density and needle penetration depth, four handsheet samples were needled, unless otherwise stated.

After the needling, the sheets were couched at Södra Cell, Sweden, in order to obtain three-ply paperboards. Before couching, the dry content of the samples was measured to be 20 ± 5%. The sheets were couched at a pressure of 400 kPa, first for 5.2 minutes and a second time for 2.2 minutes. The samples were then dried and conditioned according to EN ISO 5269-1 and EN ISO20187, with a drying time extended to 72 hours.

Grammage, thickness and density measurements

The samples were conditioned at 23 °C and 50% RH for at least 16 hours before the measurements. The grammages $\boldsymbol{w}$ of the paperboard samples and single layers were then determined gravimetrically after trimming the edges. The thickness $\boldsymbol{t}$ of the single paperboard samples and middle layers were measured for a single sheet thickness, according to standard ISO 534:1988, with a STFI thickness measuring instrument, with some exceptions. The data recorded from the thickness measurements were taken from the three single paperboard samples and middle layers prepared for each mechanical measurement. Individual samples were measured along three parallel lines and the average thickness value $\boldsymbol{t}$ and standard deviation were calculated for three samples. The density $\boldsymbol{\rho}$ was calculated according to:

$$\rho = \frac{w}{t} \tag{1}$$

The uncertainties in the grammage and density measurements $\boldsymbol{e_w}$ and $\boldsymbol{e_\rho}$ were estimated according to:

$$e_w = w_{\max} - w_{\min} = \frac{m_{\max}}{A_{\min}} - \frac{m_{\min}}{A_{\max}} \tag{2}$$

$$e_\rho = \rho_{\max} - \rho_{\min} = \frac{m_{\max}}{V_{\min}} - \frac{m_{\min}}{V_{\max}} \tag{3}$$

The estimated maximum error in the measured mass was ±0.02% and the estimated maximum error in the measured area was $\pm 25 \cdot 10^{-6}$ m^2, resulting in

nominal maximum and minimum masses m_{max} and m_{min} and areas A_{max} and A_{min}. The maximum and minimum volumes V_{max} and V_{min} were obtained by multiplying A_{max} or A_{min} by the estimated maximum or minimum thickness, calculated by adding or subtracting one standard deviation to or from the average of measured thickness.

Bending properties

Two-point-bending and folding measurements were performed on the three-ply paperboards at 23 °C and 50% RH. The two-point bending measurements were performed with a Lorentzon & Wettre Bending Tester Code 160, recording the force F at bending angles θ of 5, 7.5 and 15° (Fig. 1), in accordance with ISO 2493-1:2010. The bending length l was 25 mm and the width of the specimen b was 38 mm, allowing 8 specimens to be cut from each paperboard sample. The average bending stiffness S_b and the bending stiffness index S_b^* were calculated according to:

$$S_b = \frac{F \cdot 60 \cdot l^2}{b \cdot \theta \cdot \pi} \quad (4)$$

$$S_b^* = \frac{S_b}{w^3} \quad (5)$$

The folding measurements were performed with a Lorentzen & Wettre Creasability tester. The paperboard samples were cut into four specimens with a width of 20 mm, and the folding force was measured on at least 6 positions on each specimen, three times for each side up, giving a total of at least 24 folding measurements for each specimen. The pneumatic clamp holding the specimen turned from 0 to 90° and a load cell at a length L of 10 mm from the clamp measured and recorded a discrete number of force values F (Fig. 1).[14] The bending moment M_b at a bending angle θ of 5° was calculated according to:

$$M_b = F_b \cdot L \quad (6)$$

The folding moment was also measured, taken as the peak bending moment M_p, calculated according to:

$$M_p = F_p \cdot L \quad (7)$$

where F_b and F_p are the corresponding force readings.

Fibre structure

The fibre structure along a paperboard fold was studied, using an automated sectioning method combined with an optical microscope. Here, one sample of each H0 and H2 were prepared and studied at the Institute of Paper, Pulp and Fiber Technology, Graz University of Technology, Austria, as described previously.[15,16] Only one section of each of the two samples was analysed.

Paperboard samples with a thickness of 450-500 µm and an area of 8 x 25 mm^2 containing the fold were cut with the long side parallel to the fold. The samples were impregnated by infiltration in a gelatine capsule, using a methacrylate-based resin type Technovit 7100 from Electron Microscopy Sciences for 5 hours, to remove the air inside the fibre network. Sections with a thickness of 4 µm were cut with a rotary microtome equipped with a diamond knife. After every third cut, *i.e.* after 12 µm, the surface of the sample stub was scanned using a 3D mobile light microscope at 20x magnification, and single images was acquired with a CCD camera. Some air, however, still remained in the specimens, seen as black bubbles in the middle of the perforated hole area. A total of 150 sections were removed, representing 1800 µm along the fold. In order to convert the single images to a composite image of the whole region of interest, the individual images were stitched with an overlap of 10% and aligned.[15,16] Two-dimensional stitching of 12 (2x6) images was used to obtain a single cross-section.

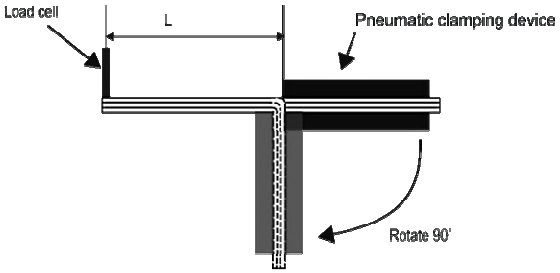

Figure 1: Experimental setup for folding and two-point bending measurements

Out-of-plane tensile strength

Strength in the thickness direction of the needled middle layer was measured according to SCAN P 80:98. Double-sided adhesive tape of type 410 from 3M was used to fix the specimens. The maximum tensile force F was recorded and the out-of-plane tensile strength σ_{ZD} was calculated according to:

$$\sigma_{ZD} = \frac{F}{A} \quad (8)$$

where the sample area A was 1000 mm^2. The standard deviation and the average value were calculated based on nine measurements.

Out-of-plane compression stiffness

Out-of-plane compression measurements were carried out on each middle layer with an MTS hydraulic machine, using specimens of 45 x 45 mm^2 in size, placed between two circular plates with an area of 1000 mm^2. The samples were preloaded to 20 N before measurement. The displacement of the samples was measured under a load at 10 kN and then after complete unloading at a rate of 200 N/s. A detailed description of the experimental set-up is given elsewhere.[17] The force-displacement data were converted into a stress-strain relationship, and analysed as described earlier.[18] The slopes of the stress-strain relationships during both loading and unloading were compared, and an elastic secant stiffness E_c was calculated based on the stress difference $\Delta\sigma$ and the strain difference $\Delta\varepsilon$ according to:

$$E_c = \frac{\Delta\sigma}{\Delta\varepsilon} \quad (9)$$

$\Delta\varepsilon$ was calculated as the difference between the strain at 4 and 8 MPa, and $\Delta\sigma$ 4 MPa. The strains measured at the compression stresses of 4 and 8 MPa were used for calculating $\Delta\varepsilon$ and the $\Delta\sigma$ was 4 MPa. The standard deviation and the average value of E_c were based on nine measurements.

RESULTS AND DISCUSSION

Bending stiffness

Figure 2 shows the bending stiffness S_b at a bending angle of 7.5 degrees for samples needled with zero, one, two and three barbs, and also the reference with no needling. The measured thickness t of each sample is shown in the figure. No significant differences in S_b were observed. A clear correlation between t and S_b was expected. This was also the case when S_b was measured at a bending angle of 5° (not shown here).

The bending stiffness index S_b^* also showed small differences between the samples (Fig. 3). S_b^*, measured at a bending angle of 7.5°, when needled with a high needle stitch density (H2 and H3), tended however to decrease with an increasing number of barbs, while having a similar grammage. There was no significant difference in density between the samples. All sample types had a density of about 760 kg/m^3 and an estimated maximal error of 40 kg/m^3. The values of t and w for the samples used are shown in Figures 2 and 3.

Folding properties

Figures 4 and 5 show the bending moment M_b measured up to 90° bending for the reference and the two needle-stitch-density groups, respectively. The initial linear slope of M_b *versus* bending angle was similar for the reference and the needled samples, but at bending angles greater than 15°, M_b depended on the needling, the difference being greater for the samples with a high stitch density (Fig. 5).

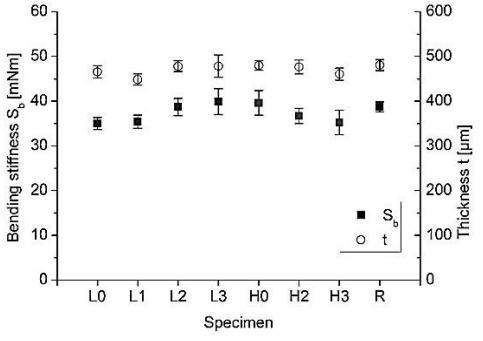

Figure 2: Average bending stiffness $\mathbf{S_b}$ measured at a bending angle of 7.5 degrees (filled symbols) and thickness **t** (unfilled symbols) for the paperboard samples with a middle layer needled with different numbers of barbs and needle stitch densities (error bars show standard deviation)

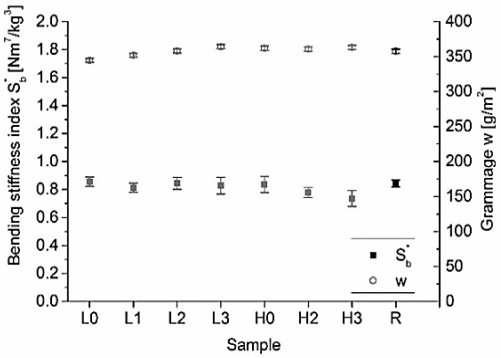

Figure 3: Average bending stiffness index $\mathbf{S_b}^*$ at 7.5 degrees (filled symbols) and grammage **w** (open symbols) for the reference (R) and the paperboard samples with a needled middle layer (error bars for **w** show the maximum estimated error and the bars for $\mathbf{S_b}^*$ show the standard deviation)

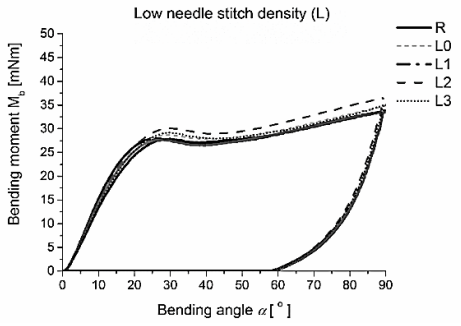

Figure 4: Measured bending moment $\mathbf{M_b}$ *versus* bending angle $\boldsymbol{\alpha}$ for paperboard samples with a middle layer needled with a low (L) needle stitch density and zero, one, two and three barbs (the solid line represents the reference sample)

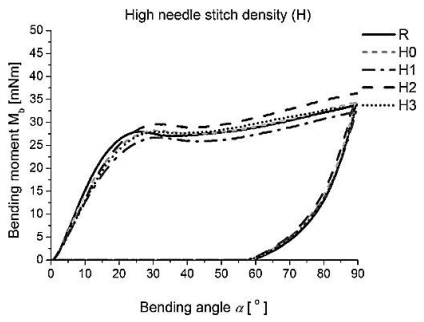

Figure 5: Measured bending moment $\mathbf{M_b}$ *versus* bending angle $\boldsymbol{\alpha}$ for paperboard samples with a middle layer needled with a high (H) needle stitch density and zero, one, two and three barbs (the solid line represents the reference paperboard)

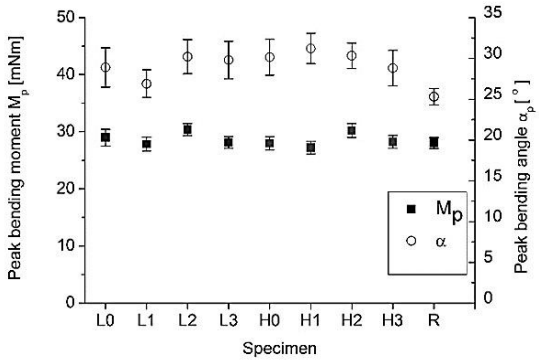

Figure 6: Peak bending moment $\mathbf{M_p}$ and peak bending angle $\boldsymbol{\alpha}$ for paperboard samples with a middle layer needled with low (L) and high (H) needle stitch density and zero, one, two and three barbs and the reference sample (R) (error bars show the standard deviation)

Interestingly, the needled samples behaved differently from the reference with regard to folding failure. Here, the peak bending moment $\boldsymbol{M_p}$ was identified as the local maximum at a bending angle between 20 and 30°, as shown in Figures 4 and 5, corresponding to folding failure. The $\boldsymbol{M_p}$ was expected to be directly correlated to the in-plane failure and the corresponding strength that occurs at the concave side of the folded paperboard.[19] Some differences in the development of the bending moment close to $\boldsymbol{M_p}$ were seen.

The values of $\boldsymbol{M_p}$ and the $\boldsymbol{\alpha_p}$ assessed are summarized in Figure 6. The figure shows that the largest $\boldsymbol{\alpha_p}$ was noted for H1 and that all the needled samples had a higher $\boldsymbol{\alpha_p}$ than the reference, but also that the differences between the needled samples were not significant, except for the rather small differences between L1 and H1. L2 had significantly higher $\boldsymbol{M_p}$ values than the reference sample, while H2 had the highest $\boldsymbol{M_p}$ and a significantly higher value than the reference. The $\boldsymbol{M_p}$ was here reached at a larger peak bending angle for L0 and L2 than for L1 and L3.

There was no significant difference between L1 and H1 in values of $\boldsymbol{t}$, $\boldsymbol{w}$ or $\boldsymbol{\rho}$, but for L2 and H2, $\boldsymbol{\alpha_p}$ was about 20% higher and $\boldsymbol{M_p}$ 8% higher than the values for the reference sample.

There were no significant differences between the samples used in the folding measurements. The thickness $\boldsymbol{t}$ was about 480 µm with a standard deviation of 18 µm or less and the density $\boldsymbol{\rho}$ was about 750 kg/m^3 with an estimated maximum error of 32 kg/m^3. With regard to grammage $\boldsymbol{w}$, the samples were divided into two populations, L0, L2, H2 and the reference had a value of about 370 g/m^2, the samples L1, L3, H0, H1 and H3 had a value of about 355 g/m^2. The estimated

maximum error in w for both sample populations was 3 g/m^2.

Fibre structure

Figure 7 shows photomicrographs of cross-sections of the three-ply paperboard samples used in the fold measurements: on the left, the sample with a middle layer needled at a high stitch density without barbs (H0) and on the right, the sample needled with two barbs (H2). The outer layers and the needled middle layer can be identified by their different fibre distributions. It can be seen that the needling reoriented the fibres in some regions close to the penetrated hole. A denser local area was seen in both samples, but in H2 some fibres were also tilted in the thickness direction, as discussed previously.[12] In H0, the fold, as well as the strained top layer, can be seen. On the right hand side of the sample, the bulged area of the compressed layer can be seen. Delamination, usually seen at the interface between the plies, was insignificant in H0. In H2 (on the right), the fold seen occurred in the denser local area, and the delamination at the interfaces between the middle and outer layers can be clearly seen.

The reorientation of some of the fibres in the out-of-plane direction, as well as the creation of locally denser areas of the fibre network may be the main reason for the higher M_p and α_p. The reorientation of fibres and denser fibre network increase the deformation resistance, which is discussed in previous work,[12] and may explain the higher compression stiffness in the out-of-plane direction for the needled samples. It is commonly accepted that an increased compressive stiffness in the out of plane direction of a middle layer should increase the bending stiffness of a paper board.[12] The difference in preparation history between the reference and the needled samples may also play a role, such as the compression during the needling of the wet fibre network.

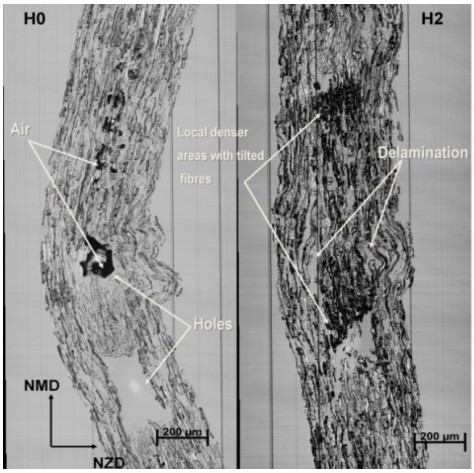

Figure 7: Optical micrographs of paperboard samples with a middle layer needled at high stitch density and with no barbs (H0) to the left and with two barbs (H2) to the right. Both samples were folded, showing the fibre orientation and the bulged structure. Delamination can be seen in H2, whereas H0 shows negligible delamination

Studying the fibre structure around the fold in Figure 7 reveals the folding took place at different positions relative to the needle penetration, leading to different deformation patterns in samples H0 and H2. The fold in H0 was located at a hole, whereas the fold in H2 was located in a denser local region with tilted fibres seen in a dark colour. The empty space from the needled hole of H0 probably enabled the compressed surface layer to move inwards more easily, resulting in a large bulged area and the release of tension in the opposite surface layer, which was not seen in H2. The delamination in H2 was probably due to the denser local area and restricted space for the compressed layer to move and release the tension in the opposite layer.

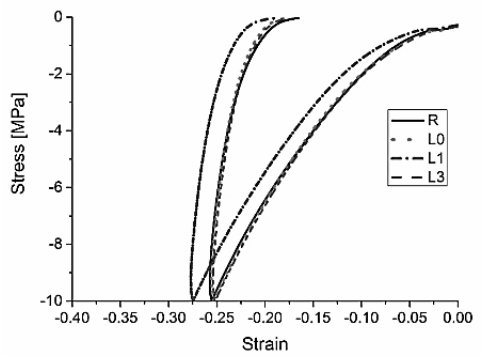

Figure 8: Stress-strain relationship during compression of middle layers needled with low stitch density and with zero (L0), one (L1) and three (L3) barbs, and of the reference (R)

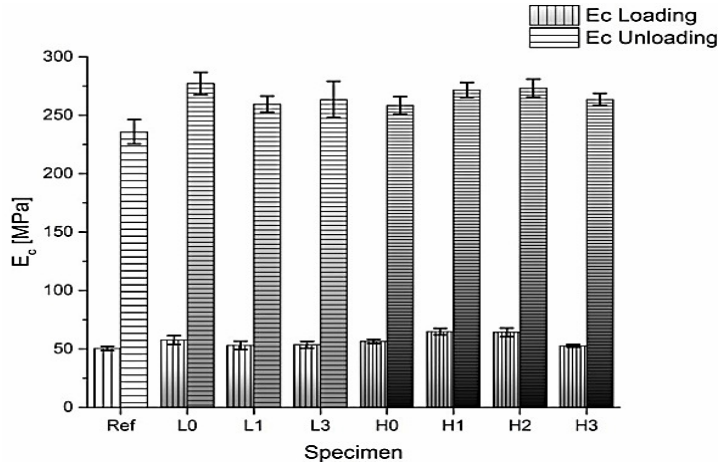

Figure 9: Elastic secant stiffness $\mathbf{E_c}$ during both loading and unloading in compression in the out-of-plane direction, defined as the difference in strain at compressive stresses of 4 and 8 MPa, for paperboard samples with a middle layer needled with low (L) and high (H) needle stitch density and zero, one, two and three barbs and for the reference sample (R) (error bars show the standard deviation)

Out-of-plane tensile strength

There were no significant differences in tensile strength in the out-of-plane direction σ_{ZD} between the needled samples and the reference. The average σ_{ZD} values were within 243 and 306 kPa, with overlapping standard deviations of about 50 kPa. No further details are given here, but it can be mentioned that there were no significant differences between the samples in terms of thickness, density or grammage, except for H2, which had a significantly higher grammage (156 ± 1 g/m^2) than that of the reference (148 ± 1 g/m^2). Note that these measurements were made on the middle layer samples, not on the three-ply paperboard samples.

Out-of-plane compression stiffness

Typical stress-strain curves during compression of the middle-layer samples with a low stitch density and the reference are shown in Figure 8. The samples produced at a high stitch density showed similar behaviour (not shown here). All recorded traces exhibited a strain hardening on compression, followed by a strain weakening on unloading.

The elastic secant stiffness $\boldsymbol{E_c}$ under both loading and unloading is shown in Figure 9. Compared to the reference, all the needled samples had a higher average $\boldsymbol{E_c}$ under both loading and unloading. The increase in $\boldsymbol{E_c}$ under loading was insignificant for samples L1, L3 and H3, but was quite prominent for samples L0, H0, H1 and H2. The highest $\boldsymbol{E_c}$ on loading, of about 65 MPa, was noted for samples H1 and H2, which was a value about 30% higher than that of the reference (50 MPa).

The $\boldsymbol{E_c}$ on unloading was, however, significantly higher for all the needled samples

than for the reference. Samples L0, H1 and H2 had a somewhat higher E_c on unloading than the other samples, about 274 MPa, which was 16% higher than that of the reference (236 MPa).

Here also, the measurements were made on the middle layer samples, not on the three-ply paperboard samples. All the samples used had a thickness of about 212 µm with a standard deviation of 13 µm or less, except for H1 that had a lower thickness t of 187 µm with a standard deviation of 9 µm. Insignificant differences were seen in the densities of the samples; as all the values were around 680 kg/m^3 and with an estimated maximum error of 51 kg/m^3. Samples L0, L3, H0 and the reference had an average grammage of about 146 g/m^2 with an estimated maximum error of 2 g/m^2, while samples L1, H1, H2 and H3 had an average value of about 137 g/m^2 with an estimated maximum error of 2 g/m^2.

It is difficult to interpret the results of the out-of-plane compression tests, as the initial elastic compression was greatly influenced by the surface roughness and may not therefore be fully representative of the material.[18] The intention was, however, to see whether there was any difference between the stress-strain curves for specimens needled with different numbers of barbs and the reference. At a low needle stitch density, all the needled specimens, except L1, exhibited loading/unloading curves similar to that of the reference (Fig. 8). Specimen L1 exhibited a flatter curve, indicating that this material was more compressible, with the same shape, than the other specimens. A low density is expected to give a more compressible material, which agrees with the fact that the density of L1 was 649 kg/m^3, compared to the density of 697 kg/m^3 for the reference. This cannot however be the only reason, since both L0 and L3 had a lower density than the reference, but exhibited a similar deformation behaviour.[17]It would be interesting in the future to study the influence of fibre length, type of needle, stitch density and the contact time between the needle and fibre structure. It would also be interesting to use thicker needles and more aggressive barbs.[20] It is however known that forming in a wet state facilitates a faster fibre network relaxation and prevents the development of internal stresses.[21]

CONCLUSION

The main result of this work was that the folding moment of the paperboard produced with a middle layer, needled with two barbs, was 8% higher than that of the reference paperboard samples with a conventional not needled middle layer. Also, the peak bending angle increased with 20% for samples needled with two barbs.

The improvement in the folding moment and peak bending angle may be explained by the increased compressive stiffness in the out-of-plane direction. An increase in the elastic secant stiffens by up to 20% during both loading and unloading was seen for all the needled samples. No significant influence of the needling on the tensile strength in the out-of-plane direction was seen.

Finally, no significant difference in either bending stiffness or bending stiffness index was noted between the needled samples and the reference.

ACKNOWLEDGEMENTS: The authors acknowledge VINNOVA (Swedish Government Agency for Innovation System) for financial support and also Södra Cell, Tetra Pak and Korsnäs for financial support, valuable discussions and experimental assistance. The authors also thank the Innventia research institute for kindly providing access to their equipment. Thanks are due to Dr A. Bristow for the linguistic revision.

REFERENCES

[1] N. Stenberg, *J. Pulp Pap. Sci.*, **30**, 22 (2004).
[2] J. M. Considine, D. W. Vahey, R. Gleisner, A. Rudie, S. R. Du Roscoat *et al.*, *Tappi J.*, **9**, 25 (2010).
[3] O. Girlanda, N. Hallbäck, S. Östlund and J. Tryding, *J. Pulp Pap. Sci.*, **31**, 100 (2005).
[4] M. Nygårds and J. Malnory, *Nord. Pulp Pap. Res. J.*, **25**, 366 (2010).
[5] C. Fellers, in "Paper Structure and Properties", edited by J. A. Bristow and P. Kolseth, Marcel Dekker, Inc., New York, 1986, p. 281.
[6] T. J. Cichoracki, E. Gullichsen and H. Paulapuro, *Tappi J.*, **84**, 61 (2001).
[7] E. A. Aaltio, *Sven. Papperstidn.*, ***3***, 58 (1960).
[8] M. Hasuike, T. Kawasaki and K. Murakami, *J. Pulp Pap. Sci.*, **18**, J114 (1992).
[9] T. Uesaka, in "Handbook of Physical and Mechanical Testing of Paper and Paperboard", Marcel Dekker Inc., New York, 1984, vol. 1, p. 640.
[10] T. Waris, *Pap. Technol. Ind.*, **31**, 14 (1990).
[11] B. Attwood and G. Moore, "An Introduction to the Theory and Practice of Multiply Forming", PiraTechnology Series, Edgerton Publishing Services, Huddersfield, UK, 1995.
[12] M. Klingberg, Licentiate Thesis, Chalmers University of Technology, 2013.
[13] Anonymous, *Pap. Technol. Ind.*, **49**, 23 (2008).

[14] H. Huang and M. Nygårds, *Nord. Pulp Pap. Res. J.*, **26**, 452 (2011).
[15] H. Schäffner, PhD thesis, Graz University of Technology, Austria, 2012.
[16] M. Wiltsche, M. Donoser, J. Kritzinger and W. Bauer, *J. Microsc.-Oxford*, **242**, 197 (2011).
[17] M. Nygårds, *Nord. Pulp Pap. Res. J.*, **23**, 432 (2008).
[18] N. Stenberg, C. Fellers and S. Östlund, *J. Pulp Pap. Sci.*, **27**, 213 (2001).
[19] S. I. Cavlin, *J. Pulp Pap. Sci.*, **1**, 77 (1988).
[20] M. Miao, H. E. Glassey and M. Rastogi, *Text. Res. J.*, **74**, 485 (2004).
[21] P. Miettinen, PhD thesis, University of Jyväskylä, 2009.